Why is the Ligurian Basin (Mediterranean Sea) seismogenic? Thermomechanical modeling of a reactivated passive margin

N. Béthoux, E. Tric, J. Chery, M.-O. Beslier

Why is the Ligurian Basin (Mediterranean Sea) seismogenic? Thermomechanical modeling of a reactivated passive margin

Nicole Béthoux,[1] Emmanuel Tric,[1] Jean Chery,[2] and Marie-Odile Beslier[1]

Received 14 November 2007; revised 15 April 2008; accepted 26 June 2008; published 24 October 2008.

[1] The seismic activity of the Ligurian Basin, the northeastern termination of the western Mediterranean basin, is larger than in surrounding regions, even though recent geodetic studies attest that this area is subject to very low levels of deformation. This basin is an example of a type of passive margins that cannot be considered solely as inert sites of sedimentation and of progressive subsidence and that are reactivated in a compressive pattern; other examples include the Kwanza basin (Angola) and the Brazil margin. We investigated, by means of 2-D thermomechanical modeling, the structural and rheological heterogeneities that can lead to concentration of strain in this marginal basin. We deduced that the deformation of the basin is due to its particular geometric features, narrow and with a thick surrounding continental crust, related to its position at the southern termination of the Alps. This sharp transition, in terms of both geometry and rheological contrast, is a main factor in explaining the weakness of the margin. We discuss the importance of buoyancy forces versus tectonic forces, as well as thermal effects, on the observed reactivation. Influence of contrast in rheology between an oceanic-type crust and continental crust is also studied. Geodynamical implications are proposed for the region. The good agreement between the predicted localized deformation and the observed seismicity distribution should help improve seismic hazard assessment in the region.
Citation: Béthoux, N., E. Tric, J. Chery, and M.-O. Beslier (2008), Why is the Ligurian Basin (Mediterranean Sea) seismogenic? Thermomechanical modeling of a reactivated passive margin, *Tectonics*, *27*, TC5011, doi:10.1029/2007TC002232.

1. Introduction

[2] Major earthquakes can occur with long recurrence times in stable continental regions that are subjected to low amounts of deformation. Understanding the occurrence of these earthquakes has long been recognized to be a complex problem.

[3] This paper addresses an example of such behavior in the Ligurian Basin, the northeastern termination of the western Mediterranean basin (Figure 1). The seismic activity of this basin is moderate, with regularly recorded magnitude 4 earthquakes and with instrumental and historical activity limited to earthquakes with maximum magnitudes on the order of 6–6.5. Nevertheless, the seismic activity of the region is significantly higher than that of surrounding regions, including the southwestern Alps, the northern Apennines, and the Corsica-Sardinia block (Figure 1). Earthquakes in the basin can be disastrous because its northern coast, the French and Italian Riviera, is a densely populated region that is characterized to large site effects [*Courboulex et al.*, 2007]. Our aim is to understand why earthquakes can occur in this area which is surrounded by regions of exclusively microseismic activity and in which the regional strain is known to be very low [*Calais et al.*, 2000]. Therefore, in an attempt to better understand the seismicity and present-day geodynamical state of this basin, we investigated, by means of 2-D thermomechanical modeling, the structural features and rheological heterogeneities that can give rise to strain accumulation. We also addressed the analogies between this basin and other passive margins that are similarly reactivated in compression.

2. Regional Geodynamical Context

[4] The recent geodynamical setting of the Alpine–western Mediterranean regions is controlled both by the African-European convergence and by subduction rollback below the Apennines [*Jolivet and Faccenna*, 2000]. The Ligurian Sea is a marginal basin that was created in the Oligocene [*Rehault et al.*, 1984; *Gueguen et al.*, 1998], during an initial stage of this trench retreat [*Doglioni et al.*, 1997]. According to *Gueguen et al.* [1997], a lithospheric boudinage effect should be responsible for the creation of several other back arc basins created in the Western Mediterranean Sea. Several studies [e.g., *Faccenna et al.*, 2004; *Goes et al.*, 2004] have highlighted the very recent changes in the geodynamical state of the Alpine–western Mediterranean regions. According to *Goes et al.* [2004], a major reorganization in the central Mediterranean occurred around 0.8–0.5 Ma, when rapid slab migration and consequent Tyrrhenian back-arc extension stopped. In correlation with this, GPS data show that the present-day oblique convergence in the western Mediterranean between Africa and stable Europe is mostly accommodated by transpressional

[1] Géosciences Azur, Université de Nice Sophia-Antipolis, IRD, CNRS, Pierre et Marie Curie Université, Paris, OCA, Villefranche sur Mer, France.
[2] Laboratoire de Géophysique et Tectonique, UMR252-43, Université Montpellier II, CNRS, Montpellier, France.

0278-7407/08/2007TC002232

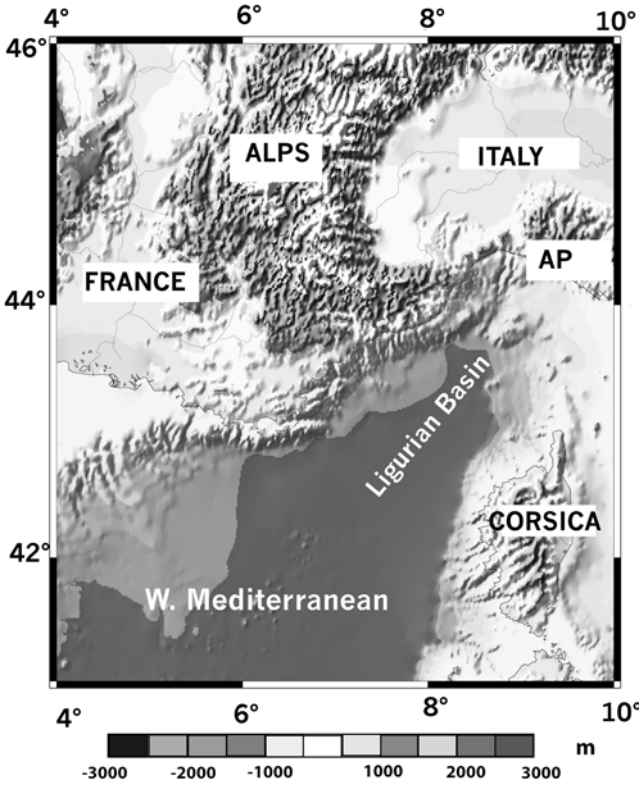

Figure 1. Bathymetry of the Ligurian Basin and topography map of surrounding regions.

deformation in north Africa and southern Iberia [*Nocquet and Calais*, 2004]. A consequence of this geodynamical change is that the western Alpine system now appears to be in a postcollisional state and to be mainly subjected to gravitational body forces [*Sue et al.*, 1999; *Delacou et al.*, 2004a]. An extension into the inner sector of the north Apennines has also been recognized [*Selvaggi and Amato*, 1992; *Serpelloni et al.*, 2005].

[5] Several modeling studies have been carried out to investigate the parameters of this evolution. *Delacou et al.* [2004b] used a simple model of the lithosphere to show that the Alpine chain is characterized by a globally extensive pattern. *Jimenez-Munt et al.* [2005] recently performed a more accurate modeling of the Alps, showing that the modern postcollisional deformation can be described without any convergence between Adria and Europe over the last 0.2 Ma. They highlight the major effect of the lateral variations in gravitational potential energy and conclude that a nonlinear strain rate-dependant rheology is required to reproduce the correct shape of the Alps. They also show, in good agreement with *Calais et al.* [2002], that a still active rotation of Adria respect to Europe is needed to explain the present-day stress field both in Western and Eastern Alps.

[6] However, although surrounded by regions recognized to be dominated by extension, the Ligurian Basin seems to be paradoxically reactivated in compression, as suggested by the presence of inverse faulting and transpression focal mechanisms [*Béthoux et al.*, 1992; *Eva and Solarino*, 1998; *Baroux et al.*, 2001]. Moreover, evidence of surrection and of compressional features is found on seismic reflection profiles along the upper northeastern margin east of Nice up to Imperia [*Bigot-Cormier et al.*, 2004].

[7] However, the GPS data, from the Provençal coast to the Corsican coast fail to show clear evidence of integrated shortening between the two margins [*Vigny et al.*, 2002]. However, *Nocquet and Calais* [2003] propose a maximum 0.5±0.5 mm a^{-1}, north-south to northwest–southeast compression in the external southwestern Alps, from station GRA, just close to Antibes, to station AJAC, in Corsica (Figure 2) with uncertainties equal to the tectonic signal detected.

[8] The Ligurian Basin, located in the Alpine-Apenninic system, therefore displays a typical behavior that we have attempt to understand better using thermomechanical modeling.

[9] The modeling studies cited above address the behavior of the whole lithosphere, at a large scale, in order to study the global geodynamics of a broad region in three dimensions. We chose to work at a smaller scale in order to look for correlations between strain distribution and the location of seismicity. We therefore modeled two representative cross sections which structures are constrained by structural features deduced from 2-D seismic lines (Figure 2). Starting from structural, gravity and heat flow data, we first analyzed the resulting strain distribution as depending from boundary forces. Then we analyzed the influence of rheologic parameters and also this one of some structural features (sedimentary thickness and Moho slope).

3. Structural and Geophysical Settings

3.1. Structural Setting

[10] The Ligurian Basin width deceases from 250 km at its southern termination to 160 km in its middle, and is surrounded by high Alpine, Apennine, and Corsican topographies. The continental margins show strong changes in width and structure along strike and on both sides of the sea, while the basin reaches a depth of 2500 m at its deepest part. This results in very marked onshore/offshore transitions, corresponding in depth to strong heterogeneities at the crustal and lithospheric scales. The Moho is uplifted at a depth of 12.5 km in the basin, whereas it deepens to 50 km under the core of southwestern Alps [*Waldhauser et al.*, 1998; *Thouvenot et al.*, 2007]. Under the Corsican margin, the slope is less steep [*Chamot-Rooke et al.*, 1999]. The deeper structure is characterized by a large-scale high of the asthenosphere [*Panza et al.*, 1980; *Solarino et al.*, 1996], which reaches a depth of 70 km in the southern central Ligurian Sea.

[11] The structure of the basin has been documented by extensive seismic data [*Rehault et al.*, 1984; *Ginzburg et al.*, 1986; *Chaumillon et al.*, 1994; *Contrucci et al.*, 2001; *Rollet et al.*, 2002]. The interpretation of these data has allowed the identification of a transitional zone, located between both margins and the basin, that is characterized by a velocity layer of 7.2–7.3 km s^{-1} over the Moho. At the center of the basin, the velocity profile has been interpreted

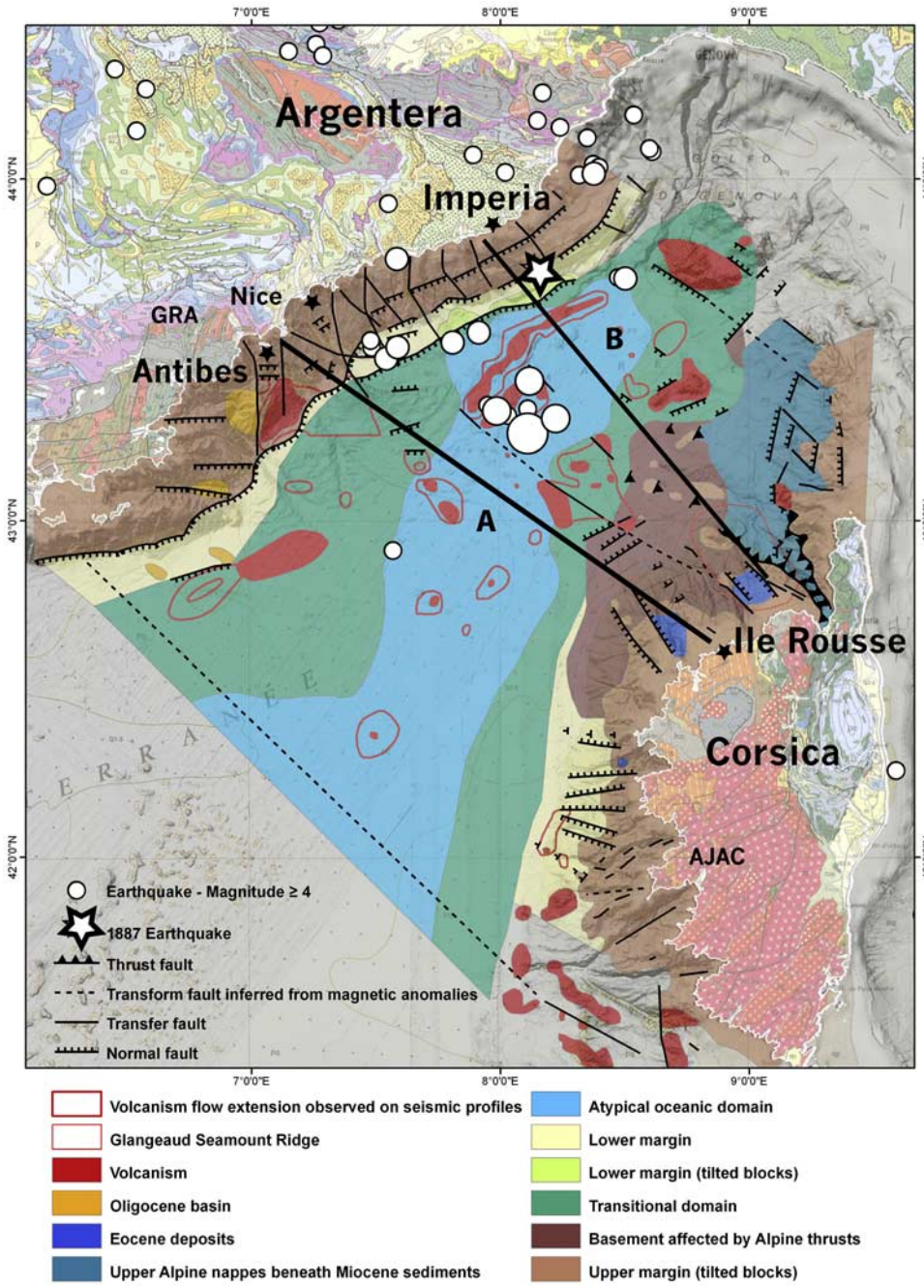

Figure 2. Structural sketch map of the Ligurian domain, after *Rollet et al.* [2002]. The seismic events of magnitude >4 are superimposed (period 1962–2001 from Bureau Central Sismologique Français catalog). The map clearly shows the asymmetry of the distribution. The Imperia historic event of 1887 (intensity X) is indicated with a white star. The two study profiles are depicted. Profile A is a cross section between the Provençal coast and western Corsica. Profile B is a cross section between Imperia (Ligurian coast) and northern Corsica. GRA and AJAC are GPS permanent stations.

as an oceanic-type crust [*Contrucci et al.*, 2001], although it could contain exhumed serpentinized mantle rather than being a typical oceanic crust [*Rollet et al.*, 2002]. Figure 2 presents the structure of the basement and the spatial distribution of the main acoustic units.

[12] Even though the main structural features of the basin have been well documented, the different seismic surveys that have been carried out have failed to obtain a clear crustal faulting image structure. This is due (1) to the presence of a thick salt layer, which creates an acoustic

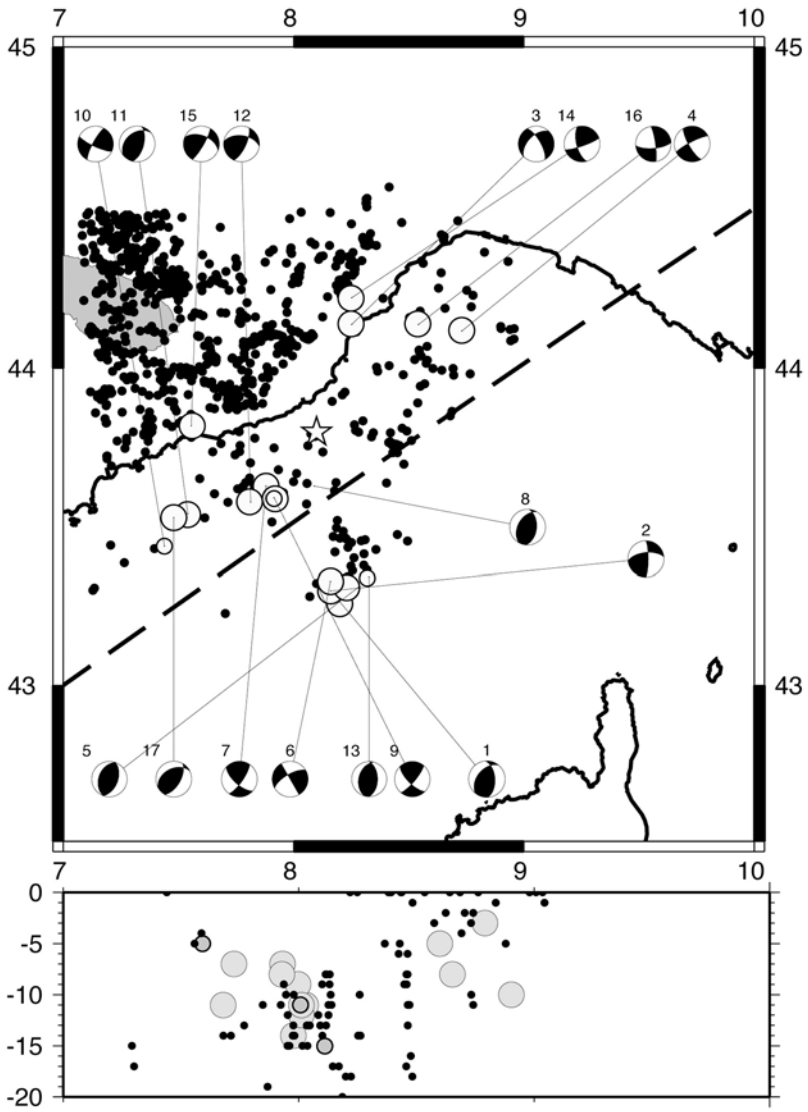

Figure 3. (a) Map of some relocated events with focal mechanisms. The black dots are the events relocated through a local earthquake tomography [*Eva et al.*, 2001], and the white circles are the events studied in several papers [*Bertil et al.*, 1989; *Béthoux et al.*, 1992, 1998; *Courboulex et al.*, 1998, 2007; *Baroux et al.*, 2001]. (b) W-E depth cross section of the hypocenters located in a 25 km wide stripe and orthogonally projected onto the section. Location of this cross section is indicated by a dashed line in Figure 3a.

velocity inversion at depth, and (2) to the time of arrival of the first water column multiple from the seafloor, as it comes close to the top of the acoustic basement reflector.

[13] The great accumulation of postrift sediments (up to 8 km thick at the foot of the northern margin) indicates that the basin has undergone remarkable subsidence. The main features of the basin may be considered as relatively stable since the Messinian Salinity Crisis period (−4 Ma). The recent subsidence is mainly due to overloading by products of erosion from the Alps and Corsican mountains, about 600 m ± 200 m over 4 Ma [*Savoye and Piper*, 1991; *Rollet*, 1999; *Chamot-Rooke et al.*, 1999] but also due to remanant cooling of the lithosphere, which has not yet reached the post rift thermal equilibrum because of the effect of rifting [*McKenzie*, 1978; *Royden and Keen*, 1980; *Sclater et al.*, 1980]. The stretching factor of crust, the thinning factor of lithosphere, the horizontal sizes of the basin and the thermal diffusivity have been already studied in the case of Ligurian Basin [*Pasquale et al.*, 1996; *Chamot-Rooke et al.*, 1999].

3.2. Seismicity

[14] Destructive earthquakes are known to have occurred in the region in historical times [*Boschi et al.*, 1995]. In this paper, we focus on the location of the Imperia earthquake, the largest studied event which occurred on 23 February 1887 and had an estimated magnitude up to 6.5 [*Capponi et*

Table 1. Rheology Parameters Used in the Modeling

Name	Continental Crust	Transitional Crust	Oceanic Crust	Sediments	Upper Mantle
Density (kg m^{-3})	2660	2750	2900	1650	3100
Young modulus (Pa)	2×10^{11}	4×10^{11}	5×10^{11}	2×10^{11}	5×10^{11}
Poisson ratio	0.25	0.25	0.25	0.25	0.25
Cohesion	10^7	10^7	10^7	10^6	10^7
Internal friction angle (deg)	20	20	20	15	20
Power law strain rate (Pa^{-n} S^{-1})	10^{-22}	10^{-22}	7.5×10^{-17}		7.5×10^{-17}
Power law exponent	3.4	3.3	3.3		3.3
Activation energy (kJ mol^{-1})	139×10^3	300×10^3	444×10^3		520×10^3
Thermal conductivity (W m^{-1} K^{-1})	3.0	2.8	3.0	1.5	3.0
Specific heat (J kg^{-1} K^{-1})	1070	1070	1070	1070	1070
Heat production (W m^{-3})	2.5×10^{-6}	1.5×10^{-6}	1.5×10^{-7}	1×10^{-6}	1×10^{-8}

al., 1980; *Ferrari*, 1991; *Scotti et al.*, 2007] as well as on the 19 July 1963 event of magnitude 5.9–6.2 [*McKenzie*, 1972; *Béthoux et al.*, 1998]. We also consider the magnitude 4–4.5 shocks that are regularly recorded with an approximate period of 2–3 years (Figure 2). One important feature of the activity in the basin is that the seismicity is concentrated in its northern part. In contrast, the southern margin and Corsica are quite aseismic (with only some sparse, very low magnitude events occurring there). Older events in the Ligurian Basin are ill localized, mainly in terms of depth, because all the stations were operating along the coast of Liguria and France. The densification of networks, the installation of stations in Corsica, and the temporary use of OBS (oceanic bottom stations), has improved the reliability of more recent seismicity measurements. These recent locations (Figure 3a) show that focal depths of the seismic events (Figure 3b) are rather shallow, between 2 and 20 km depth [*Eva et al.*, 2001; *Courboulex et al.*, 1998, 2007]. All the computed focal mechanisms are inverse faulting or transpressive with a P axis oriented N120–N130 [*Béthoux et al.*, 1992; *Eva and Solarino*, 1998; *Baroux et al.*, 2001; *Courboulex et al.*, 2007]. They show stability of the nodal planes, which correspond to the direction of the rifting axis and to perpendicular directions, assimilated to transform faults. Figure 3a depicts the solutions obtained and details of locations and focal parameters are given in Table 2.

4. Numerical Modeling

[15] We used the ADELI code [*Hassani et al.*, 1997], which allows thermomechanical modeling in a 2-D heterogeneous medium. This finite element numerical model solves for the momentum equation, given the constitutive law of the medium and the static and kinematic boundary conditions (see *Hassani et al.* [1997] and *Chery et al.* [2001] for details about this methodology). The aim of this kind of modeling is to find the relationships between the intensity and direction of external forces and steady state deformation in the medium. This code requires the starting state of the medium to be in equilibrium before applying external forces to the medium in order to determine the evolution of the system.

[16] The reliability of the model was demonstrated by several tests: First, we tested the independence of the results from the numerical parameters, such as the mesh and time stepping, used in the computation. Second, we verified the reliability of the modeled thermal state (depth of isotherms, comparison with the present-day observed heat flow). Finally, the modeled strain was compared to existing geodynamical knowledge and to the known seismicity pattern.

[17] In our modeling, the lithosphere was assumed to behave as an elastoplastic medium at low temperatures and as a viscoelastic medium at high temperatures. Plasticity takes into account the qualitative changes in the response that a material shows to deformation when the stress is larger than a yield limit, i.e., the boundary between reversible and irreversible deformation.

[18] In the plastic domain, we used a Drucker-Prager rheology in order to take into account the increase in differential stress with pressure. Such models are defined by an internal friction angle, "f," and a cohesion, "c" [*Byerlee*, 1978; *Leroy and Ortiz*, 1989]. We used different f and c values for the different crustal domains to take into account their different rheologies, as explained below. For the continental margin, we used standard values for continental crust as provided by *Kirby* [1985]. The sediments were also considered using an elastoplastic rheology, but with low-cohesion behavior (10^5 to 10^6 Pa.). The rheology of the oceanic lithosphere has been the subject of numerous studies [e.g., *Chen and Morgan*, 1990]. Following *Chen and Morgan* [1990], we used relatively similar values for the oceanic crustal layer and the mantle. As the so-called "transitional domain" has been interpreted to be a thinned continental crust submitted to underplating resulting from the partial melting of the upper mantle [*Rollet et al.*, 2002], we characterized these blocks using intermediate rheological parameters, between the continental crust and the oceanic crust.

[19] A Maxwell model was adopted to fit the strain rate-dependant "power law" rheologies. The stress is a function

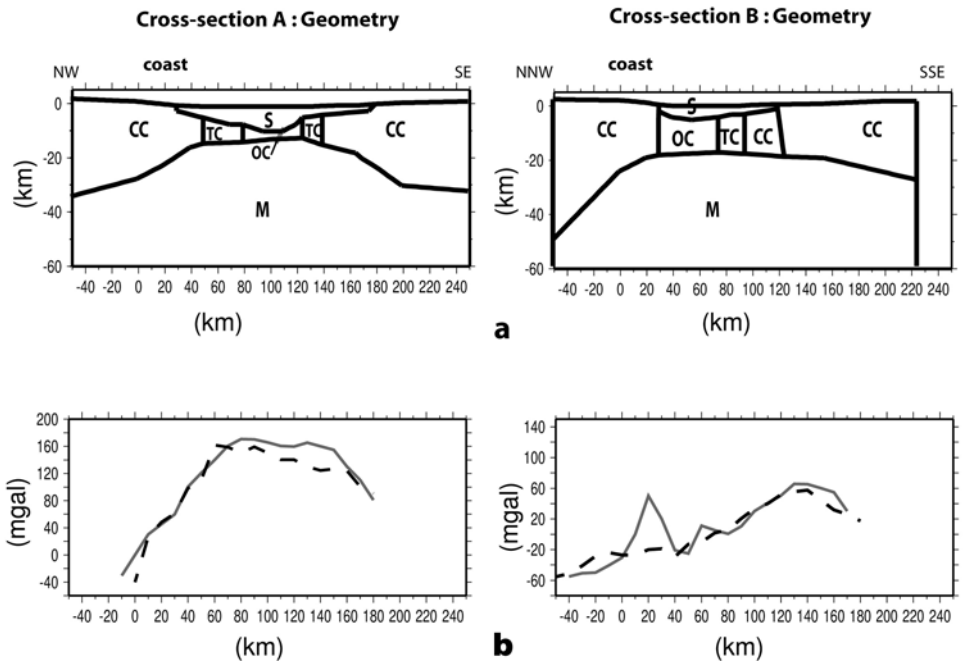

Figure 4. (a) Crustal structure used in the modeling. These structures are in good agreement with the gravity anomalies. (b) Bouguer anomaly. The continuous line corresponds to the observed values. The dashed line corresponds to the 2-D modeling of gravity anomaly.

of γ, the fluidity (inverse of viscosity), which depends on the temperature T and the activation energy such as:

$$\gamma = \gamma_0 \, e^{-E/RT}$$

where γ_0 is a multiplicative term that depends on the material, T is the temperature in degrees Kelvin, E the activation energy in Joules, and R the universal gas constant (8.314 J $mol^{-1}K^{-1}$) and γ in Pa $^{-n}$ s^{-1}.

[20] The values of γ_0 and E are given for various rocks in a review paper by *Kirby* [1985]. We also used heat production rate deduced by *Pasquale et al.* [1996] who determined the drifting stage timing of the Ligurian-Provençal basin from the heat flow data. The range of thermomechanical parameters used in the modeling is displayed in Table 1.

[21] We chose to model two structurally differentiated cross sections (Figure 2), one in the central part of the basin and another in its northeastern part. The first (A) corresponds to the seismic line studied by *Contrucci et al.* [2001]. It is approximately perpendicular to the margins and corresponds to the southern limit of the seismic swarm. We defined a simplified crustal geometry (Figure 4a), with blocks of continental crust, an oceanic domain block, and transitional blocks. The lateral limits of the blocks used were those obtained by *Rollet et al.* [2002] by correlating several seismic profiles. The sedimentary layer includes the water layer. The second modeled cross section (B) corresponds to a transverse section going from Imperia, on the Ligurian coast, to northern Corsica, and crosscutting the approximate location of the 1887 seismic event. Here, the basin is very narrow and is characterized by a steep northern margin, a lack of transitional domains (Figure 2), and high Alpine topographies that are found just near the coast.

[22] The chosen cross sections satisfy all the data available which document the major features of the structure. In addition, we used the gravity map derived from the free air gravity field of *Sandwell and Smith* [1995], the heat flow data [*Jemsek et al.*, 1985; *Della Vedova et al.*, 1995], and the thermal study of the basin [*Pasquale et al.*, 1996]. Note that the structure is compatible with the Bouguer anomalies deduced along the cross sections (Figure 4b). The observed short wavelength of the observed Bouguer anomaly corresponds to volcanic massifs (see Figure 2) and was not included in our modeling. We first verified that our starting model was in hydrostatic equilibrium, taking only the hydrostatic pressure at the bottom of the model as boundary conditions. Because we were modeling an elastoplastic behavior of the medium, we needed to impose external forces to obtain an evolution of the system. We therefore imposed a horizontal (initially chosen as shortening) velocity on the lateral boundary of the model.

[23] We tested different numbers of elements (3500, 8000, 15,000) in order to verify that the discretization did not affect the model results. We modeled the evolution of the system over a 4 Ma period, testing time steps ranging from 1.25 years to 4000 years. Regardless of the mesh and time step used, convergence was obtained and the numerical results were identical. We present below modeling obtained with 13,000 elements and time steps of 400 years.

[24] The 4 Ma period corresponds to a period beginning after the Messinian perturbation of the basin and continuing up to the present. In order to take into account the increase in the plio-Quaternary sediment thickness and the ongoing

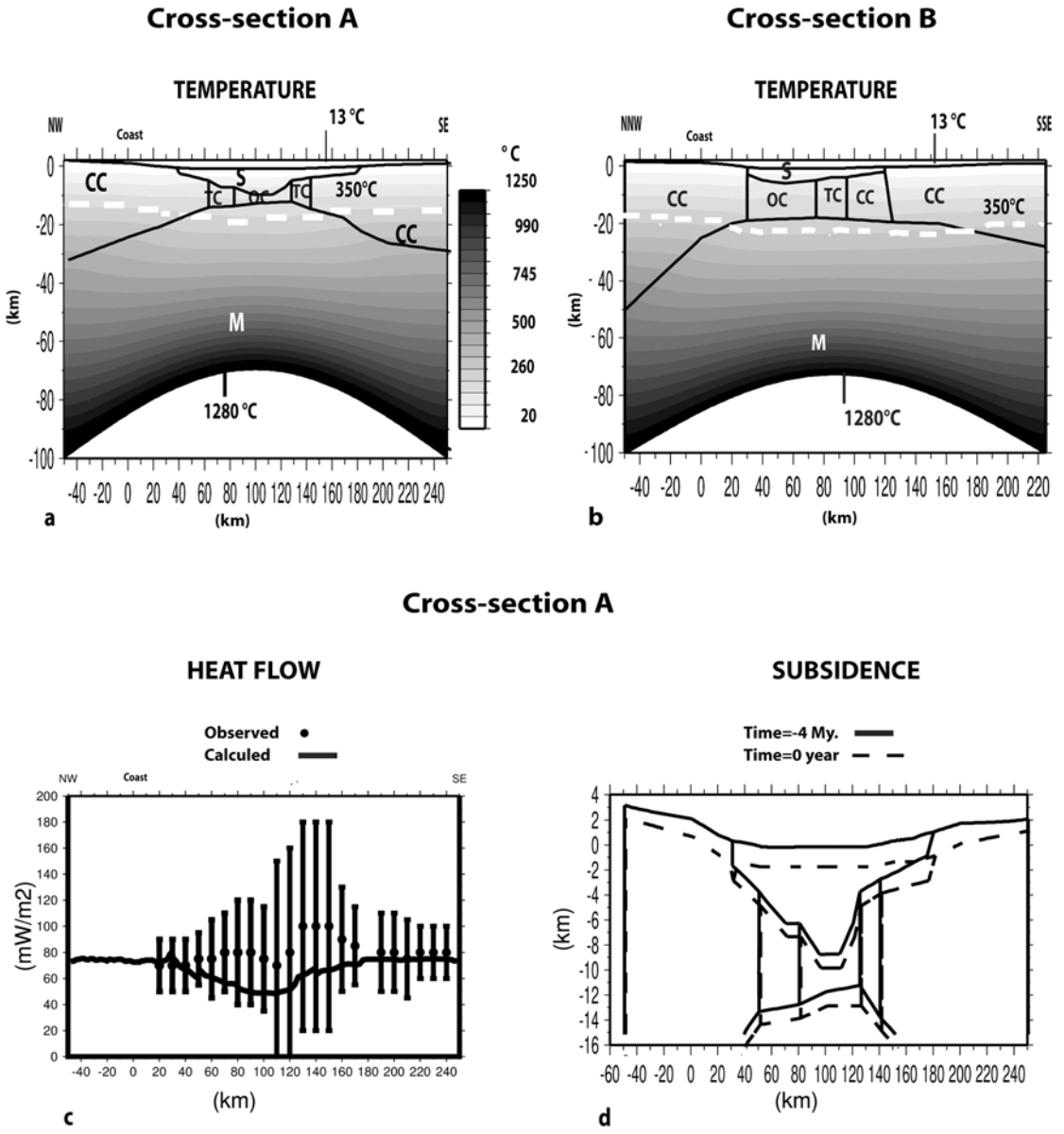

Figure 5. Temperature pattern computed after 4 Ma for (a) Profile A and for (b) Profile B. (c) The heat flow computed for the margins and at the bottom of the sedimentary layer, compared with the measured data (in circles) along Profile A. Error bars are shown. (d) Effects of erosion. The modeling corresponds to a starting time of −4 Ma, with a higher topography than today and a thinner sedimentary layer. The initial structure is drawn with a fine continuous line. The resulting structure corresponds to the dotted line.

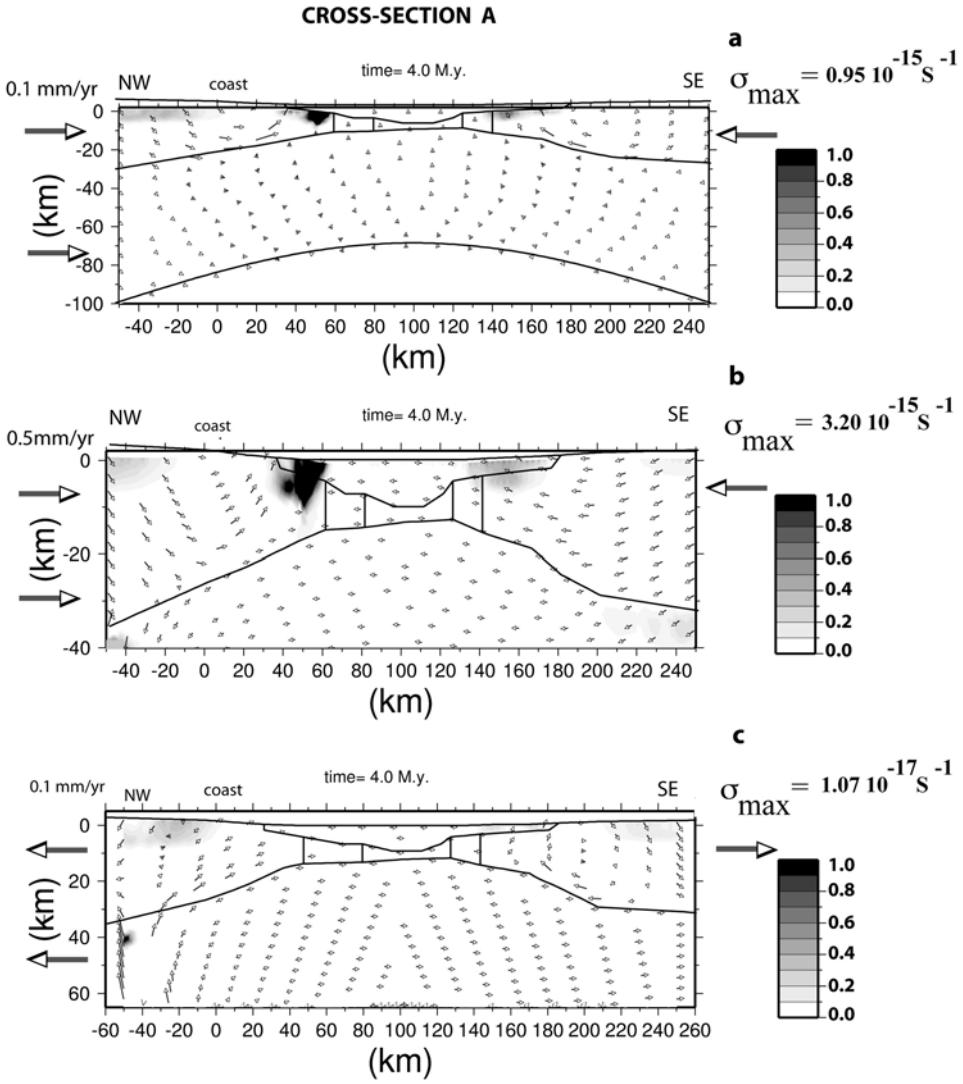

Figure 6. Profile A: (a) Results of the thermomechanical model with a convergence velocity of Vn = 0.1 mm a^{-1}. The modeling goes from the −4 Ma up to present. The intensity of deformation is plotted in gray, while the arrows indicate the displacement field. The maximum average total strain rate is indicated. (b) Result of the thermomechanical model for a velocity of Vn = 0.5 mm a^{-1}. We focus the results on the crustal structure. The maximum average total strain rate is indicated. (c) Results of the thermomechanical model for an extensive velocity of Vn = −0.1 mm a^{-1}.

subsidence, we modeled erosion on the two inland parts of the region (Figure 5c). To obtain the present-day structure, we started the modeling with a higher topography (increased by 1 km for the top of the topography), a thinner sedimentary layer (thickness decreased by 500 m), a Moho shallower of 1 km than now, and a shallower (1 km) lithosphere-asthenosphere boundary, compatible with the subsidence modeling published by *Chamot-Rooke et al.* [1999].

5. Temperature and Heat Flow

[25] Because rheology is strongly linked to the thermal state, we introduced thermal boundary conditions corresponding to a surface temperature of 13°C (which is the bottom water temperature of the Mediterranean Sea) and a temperature of 1280°C for the boundary between the lithosphere and asthenosphere, a value computed for present-day by *Chamot-Rooke et al.* [1999] on the basis of thermal/gravity modeling of the Ligurian Basin. We also used heat production rate deduced by *Pasquale et al.* [1996] who determined the drifting stage timing of the Ligurian-Provençal basin from the heat flow data. They concluded that the late Miocene period corresponds to the final phase of drifting in the northern Liguro-Provençal basin, in good agreement with others authors [*Rehault et al.*, 1984; *Jolivet et al.*, 1990; *Gueguen et al.*, 1998]. The methodology used in this study does not allow modeling the transient compo-

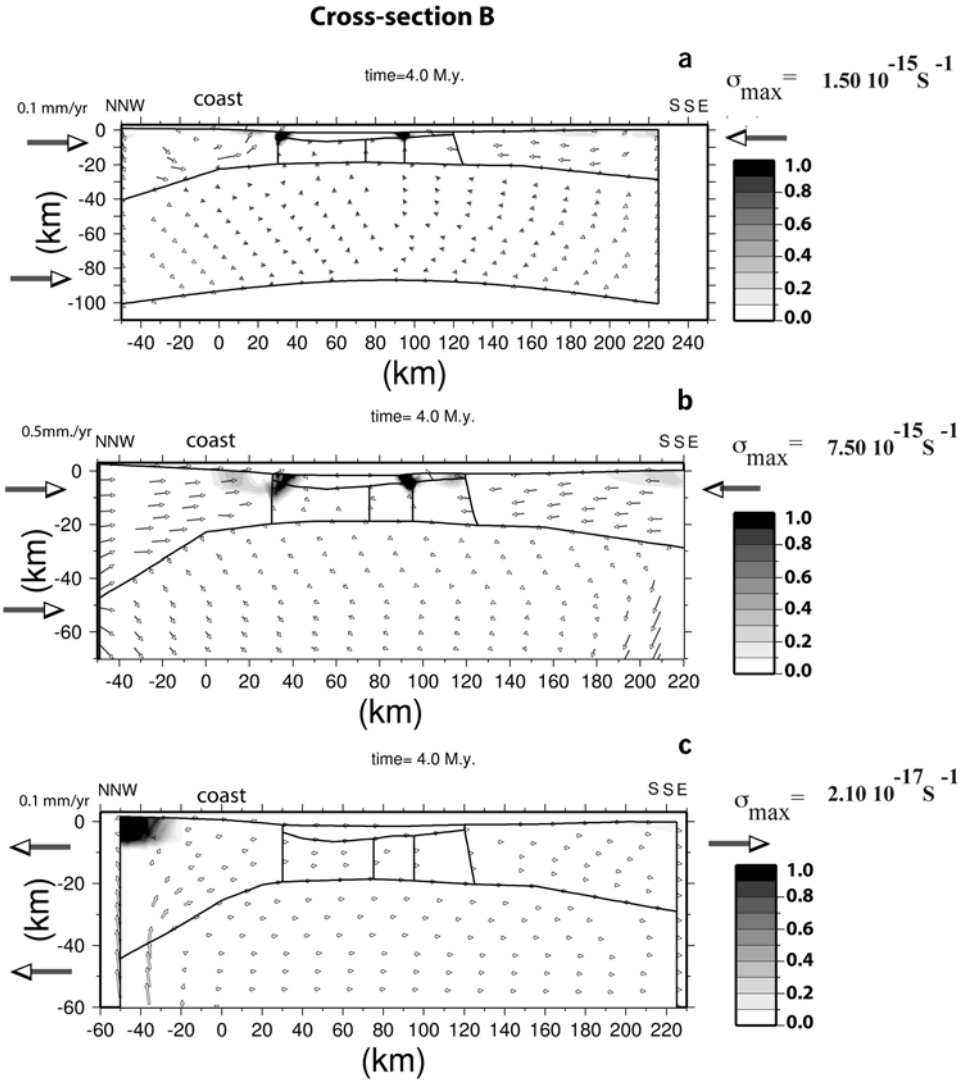

Figure 7. Profile B: (a) Results of the thermomechanical model with a convergence velocity of = 0.1 mm s^{-1}. The modeling goes from −4 Ma up to present. The intensity of deformation is plotted in gray, while the arrows indicate the displacement field. The maximum average total strain rate is indicated. (b) Result of the thermomechanical model for a velocity of Vn = 0.5 mm a^{-1}. We focus the results on the crustal structure. (c) Results of the thermomechanical model for an extensive velocity of Vn = −0.1 mm a^{-1}.

nent of heat flux which is mainly controlled by the time of rifting and the stretching amount. However, *Zito* [2005] performed a 3-D thermal modeling of small back-arc basins, as Tyrrhenian basin, or the Liguria Sea. Because this type of basin limited in space cools more rapidly, he shows that for these basins, the evolution of temperature and heat flow, after 10 Ma is not drastic over a period of 4 Ma (max 10%). We therefore assume the stationarity of thermal parameters during the modeling period. In the following, we will test the influence of variations in the values of these parameters.

[26] Moreover, our model takes into account the subsidence of the basin during the last 4 Ma which is controlled both by erosion of the mountainous inlands and by thermal adjustment of the lithosphere. (Figure 5 (days))

[27] Figure 5a shows the temperature field computed in the model for cross section A. The isotherms have a very particular shape and are strongly linked to the lithospheric thickness. The Moho temperature depicts a gradient along the profile. Under the basin, it depicts a low of the isotherms. The isotherms are deflected on the two flanks of the continental margins, with the deflection being stronger on the northern flank. For cross section B (Figure 5b), the thickness of the sedimentary layer is lower than with cross section A, and less blanketing of the heat flow occurs. *Hansen and Nielsen* [2002] studied the evolution of sedimentary basins, formed in extension and reactivated in compression, whereas the upper mantle, being shallower than before stretching, is relatively strong in comparison to

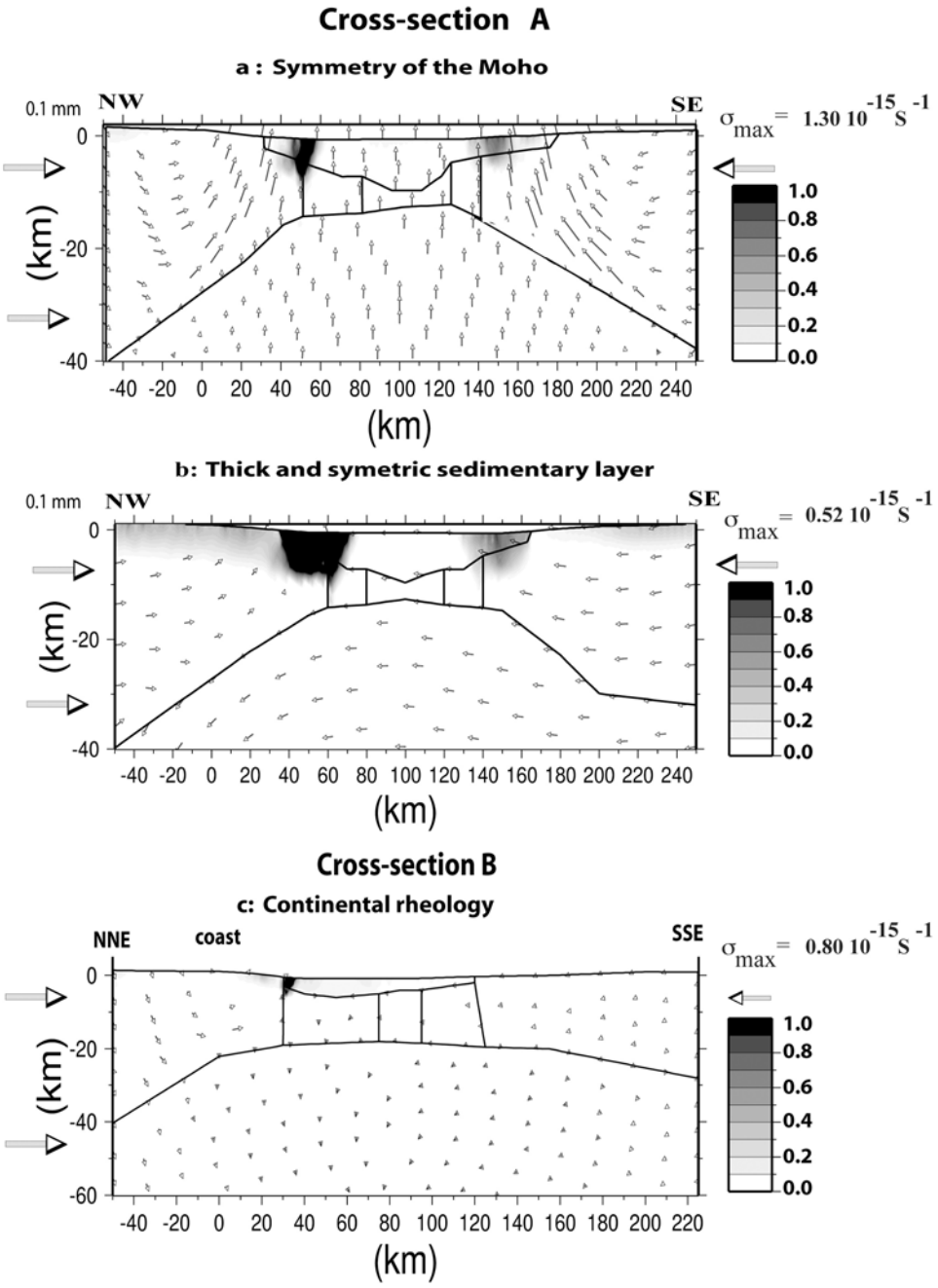

Figure 8. Profile A: influence of the asymmetry of the structures for (a) asymmetric shallow structures and symmetric Moho, for a velocity of 0.1 mm a^{-1}. (b) Symmetry of the sedimentary layer (to be compared with the geometry previously modeled in Figure 8a). Figure 8b compares the asymmetric shallow structures and symmetric Moho with the Moho topography previously modeled for the southern margin. This change has the consequence of increasing the thickness of shallow structures. (c) Profile B: modeling of a crustal structure only including a sedimentary layer and a continental crust (V = 0.1 mm a^{-1}).

the surrounding mantle under the adjacent margins and continents. Resolving the thermal equation, they show that the heat flow profile exhibits a low in the basin and a high at the margins. The deviation of heat flux is caused by heat refraction, mainly due to the conductivity contrast of sediment and upper crust. We observed a similar temperature deviation in the Ligurian Basin, facilitated by the narrow dimension of the basin and the thick sedimentary layer. This temperature distribution is also similar to this one modeled by *Zito* [2005] for the Tuscan-Tyrrhenian basin. This thermal distribution shows that the lithosphere has not yet reattained its equilibrium thickness.

[28] In Figure 5c, we present the available observed marine heat flux values corrected for sedimentation [*Della Vedova et al.*, 1995]. This correction is crude; however, as it corresponds to a constant correction factor of 30%, and thus does not take into account the accurate thickness of the sedimentary layer and the presence of salt. The modeled heat flow curve is computed across the profile, under the sedimentary layer. Both curves depict a relative minimum along the northern margin, because of the asymmetry of sediment layer. Taking into account the large error bars, our values are roughly of the same order of magnitude, mainly for the two continental margins (about 80 mw m^{-2}) but less than the observed one in the basin, because of residual thermal anomalies linked to the extensional processes [*Pasquale et al.*, 1996] and the presence of volcanic bodies [*Della Vedova et al.*, 1995], which we did not take into account in our modeling.

[29] Moreover, we note the good agreement between the focal depths of the seismic events and the range of depth of the brittle thickness (given by the isotherm 350°C), as deduced by temperature modeling for the present-day (Figures 5a, 5b, and 9).

[30] Accordingly, we conclude that the rheological parameters used allowed the modeling of a rather realistic present-day thermal state.

6. Results

6.1. Influence of Boundary Forces

[31] Starting with structural and thermal parameters as input data, we analyzed the influence of boundary forces. In view of recent geodetic results [*Calais et al.*, 2002; *Nocquet and Calais*, 2003], we imposed very low kinetic boundary conditions, in the range 0.01 to 1 mm a^{-1}, on our mechanical model in order to test the robustness of the mechanical equilibrium. For cross section A, even a low shortening velocity of 0.1 mm a^{-1} induced a localized deformation at the foot of the northern margin, between 20 km and 40 km from the coast and limited to the upper 15 km; on the other hand, a low and diffuse deformation was modeled in the sedimentary layers of the southern continental margin (Figures 6a and 6b). A deformation also appeared onshore, on the upper part of the northern continental margin. Whatever the velocity imposed as a boundary condition (as low as 0.01 mm a^{-1}), the displacement field was limited to the two continental margins, while in the basin the displacement vectors were negligible. The shortening was mainly absorbed in the margins, whereas the basin remained stable. The gray scale in Figures 6, 7, and 8 has been normalized to the maximum intensity of each experiment to better show the spatial distribution of strain. The maximum value of average cumulated strain rate is indicated in Figures 6, 7, and 8.

[32] The same process was applied to the modeling of the second cross section, B.

[33] Figure 7a presents the results of the thermomechanical modeling obtained using a horizontal boundary velocity of 0.1 mm a^{-1}. One region of deformation corresponds to the sharp transition between a thick continental crust and oceanic crust. Another patch of deformation is evidenced in the middle of the basin. The corresponding maximum strain rate reaches 7.5 10^{-15} s, which is larger than the value obtained for cross section A, 0.95×10^{-15} s^{-1} for the same boundary velocity. For 0.5 mm a^{-1} we obtain for cross section A, a maximum of total strain of 2.5×10^{-15} s^{-1} and 7.5×10^{-15} s^{-1} for cross section B.

[34] As the present-day Alpine-Apennines system is now recognized as being globally extensive [*Jolivet and Faccenna*, 2000; *Calais et al.*, 2002; *Delacou et al.*, 2004b], we also tested extensional velocities on the limits of the two models A and B. Along the two profiles (Figures 6c and 7b), the resulting strain was localized exclusively in the hinterland, corresponding to the rim of the southwestern Alps and Corsica, with the marine part of the model remaining inactive. The main effect of these extensive forces was to cause uplift of the two continental margins.

6.2. Influence of Structural Features

[35] Applying again a shortening boundary velocity, we next attempted to determine which parameters could account for the asymmetry obtained in the modeled strain distribution, mainly for cross section A, that is more typical of the regional basin structure. We first check different slopes of the Moho, between the coast and the hinterland. The distribution of deformation is unchanged but the average strain rate is increased of 20%, when the Moho depth increases from 30 km, 50 km away from the coast, as observed northwest of cross section A, up to 40 km, 50 km away from the coast, as observed north of Argentera massif [*Thouvenot et al.*, 2007] near cross section B. Then, we used in the computation a deformed basin with an approximate symmetry of the Moho and inland topography, although with unchanged asymmetric sedimentary layers, as reflected in the structural data (Figure 8a). We found that the change in body forces on the southern margin provided a more balanced strain rate between the two margins, when the Moho slope is symmetric. However, along cross section A, the northern margin was still subjected to higher strain than the southern one was, because of the asymmetry of the sedimentary layer and the upper margin. Using another structural geometry (Figure 8b), we also show that the thickness and shape of the sedimentary layer is a main factor influencing the cumulated strain value: when this thickness was increased, the strain rate drastically decreased.

6.3. Influence of Contrast in Rheology

[36] In order to test the importance of contrast in rheology of the continental crust and the oceanic crust, we model the blocks of the basin TC and OC (see Figure 4a), with rheological parameters identical of those of continental crust (CC). For both cross sections, the cumulated strain decreases of about 20%. For cross section A, the pattern of deformation remains identical. For cross section B, the deformation is only localized at the foot of the northern margin, and there is no patch of deformation as observed

Table 2. Location and Focal Solutions of Some Seismic Events[a]

Date	Time (UT)	Longitude (°N)	Latitude (°E)	Depth (km)	Ml	Strike	Dip	Rake	P Axis		Reference in Figure 3
									Strike	Dip	
19 Jul 1963	0546	8.150	43.330	14	6.0	220	46	124	107	04	1
27 Jul 1963	0557	8.160	43.340	14	4.8	264	61	168	129	13	2
30 Dec 1970	0220	8.253	44.138	05	4.0	224	52	−155	193	42	3
25 Sep 1971	1034	8.730	44.117	10	4.2	150	75	−169	107	18	4
5 Jan 1981	0810	8.230	43.311	11	3.6	200	40	90	110	05	5
22 Apr 1981	0426	8.060	43.330	09	4.5	240	68	−180	103	15	6
4 Oct 1985	1322	7.980	43.630	12	4.0	132	66	17	85	06	7
4 Oct 1985	1558	8.090	43.610	11	3.9	210	45	108	107	01	8
5 Oct 1985	1558	7.916	43.593	11	3.1	135	69	088	88	05	9
1 May 1986	0028	7.440	43.440	05	3.8	115	78	166	341	0	10
26 Dec 1989	1959	7.541	43.543	07	4.5	231	36	119	119	13	11
15 Apr 1990	0750	7.814	43.580	08	4.3	278	52	148	148	12	12
21 Sep 1992	1237	8.328	43.344	18	3.0	220	40	110	97	05	13
17 Jul 1993	1035	8.253	44.221	08	4.5	165	65	9	120	11	14
21 Apr 1995	0822	7.556	43.823	04	4.3	292	51	167	155	19	15
25 Nov 1996	1947	8.542	44.137	03	3.8	352	81	307	004	05	16
27 Feb 2001	1734	7.482	43.534	11	4.7	243	41	74	120	04	17

[a]See *Béthoux et al.* [1992], *Baroux et al.* [2001], and *Courboulex et al.* [2007].

previously in the middle of the basin at the transition between OC and TC.

6.4. Influence of Thermal Conditions

[37] Using slightly larger values of heat production factors or energy activation (10%) involve larger computed surface heat flow and total cumulated strain, (in an order of magnitude). We also introduced in the modeling, the actual heat generation known for continental stable crust (1 μW m^{-3}) and sedimentary layer (0.1 μW m^{-3}). Using these actual production factors implies that we assume the basin has reached its thermal equilibrium. This change does not modify the deformation pattern but leads to a dramatic decrease of the cumulative value of strain during 4 Ma. The maximum strain rate is lowered to be the tenth of the value obtained with the original parameters (Table 1) that allow a rather good fit of thermal modeling with observed heat flux and seismogenic thickness (depth of isotherm 320°).

7. Total Strain Distribution and Seismicity Location

[38] In this section, we address microseismicity relocation (Figure 3a) using a local earthquake tomography [*Eva et al.*, 2001] and considering the most recent M > 4 events, carefully relocated [*Courboulex et al.*, 1998, 2007; *Baroux et al.*, 2001] (Figure 3b and Table 2).

[39] In Figure 9 we provide a map with the two cross sections A and B (denoted here AA′ and BB′) and three cross sections from the tomography study of *Eva et al.* [2001] We present these cross sections from west to east. Note that our modeling, which focuses on the deformation of the Ligurian Basin, cannot explain the occurrence of earthquakes in the hinterland (close to points C and E, Figure 9a), which is subjected to the geodynamics of the Alps.

[40] Cross section EF, normal to the coast, shows the seismicity from the southwestern Alps (see Figure 9a) to the center of the basin, in a position median to our two lines A and B. Line CD is close to our cross section B. but in fact shows very few seismicity in the margin or in the basin, which could be partly explained by the short period of recorded seismicity (period 1981–1998) and by the poor azimuthal coverage of the recording stations (the ill located events are rejected in the tomography process). Profile GH is parallel to the coast and corresponds to the foot of the northern margin, where a major part of the seismicity is concentrated (Figure 2 and Figure 3a). The comparison between the two results shows the agreement in the location of the strain and the seismicity along the foot of the continental margin (the boundary between the continental crust and the transitional or oceanic crust), which corresponds to the Profile GH. The hypocenters deduced from location of seismic events and from local tomography are located between 5 and 15 km deep, up to the foot of the margin (Figure 3b); In addition, computation of the isotherm 350° between 15 and 20 km in depth and the location of the patches of strain between 5 and 15 km, at the foot of the margin, provide good arguments for the coherence of the modeling and the seismicity pattern.

[41] We can also conclude that the Imperia event, of approximate magnitude 6.5, and instrumental seismicity, occurred near the boundary between the continental margin and the oceanic domain, where the maximum strain rate was computed by our model of cross section B.

[42] It is worth noting that many events, including the 1963 event (Ml ∼ 6.0) and its aftershocks, are located along Profile EF, along the border of the sharp offset toward the north, of the oceanic domain and are slightly deeper (up to 20 km deep) (Figures 2 and 9). This region corresponds to a

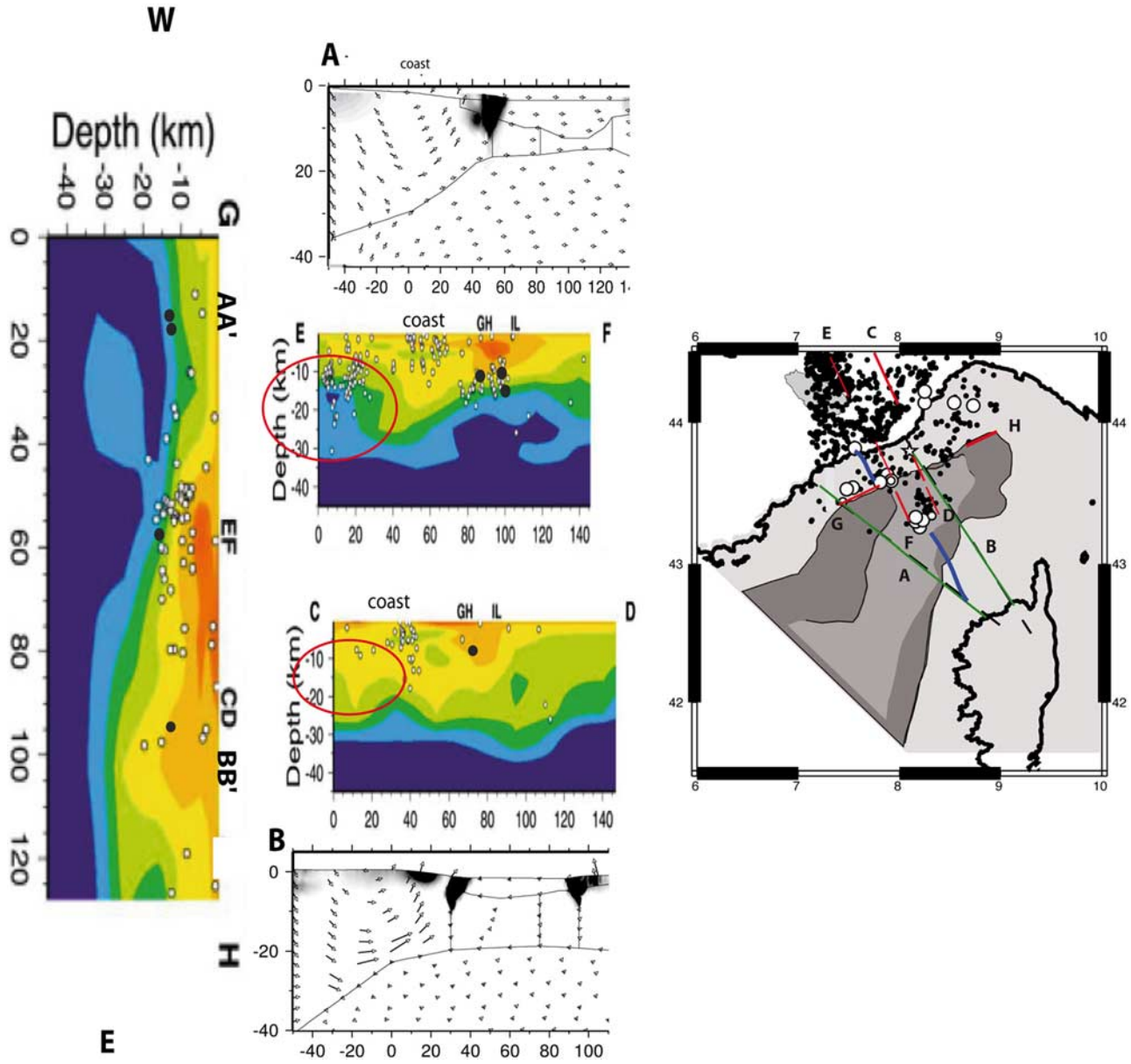

Figure 9. Comparison between seismicity and strain modeling patterns. The different cross sections are shown in the map. Green is thermomechanical modeling, and red is tomography profiles [*Eva et al.*, 2001]. The different sections are presented from west to east. The Profile EF is rather far from AA. Seismic events listed in Table 2 are projected on these cross sections, with dark circles and seismicity from tomography shown by white circles. The corresponding epicenters are in Figure 3. The red ellipse shows the seismicity that we consider associated with Alpine tectonics.

transfer zone, originally identified on the margin by *Rollet et al.* [2002], that accommodates the differential deformation between two segments of the margin. Because of the simplification in our modeling, we were not able to take into account the effect of this transform fault, which probably acts like a weakness zone. However, the results obtained for cross section B, which describes the deformation of this part of the basin, suggest that these poorly located ''old'' events likely reactivated the transition between the oceanic and transitional domains, where we evidenced a patch of deformation. Their epicenters should therefore be shifted toward the south.

8. Is the Ligurian Basin a Typical Reactivated Passive Margin?

[43] Using rather simple thermomechanical modeling, we found that even a very small shortening force applied to the

borders of the Ligurian Basin (we tested values as low as 0.01 mm a^{-1}) is sufficient to produce strain localization, mainly at the foot of the northern continental margin and to a lesser extent at the boundary between the oceanic and transitional domains, where the basin becomes narrowest and where the sedimentary layer is rather thin. In the following we discuss the different causes that lead to a reactivation of this basin.

[44] As recently stressed by *Hudec and Jackson* [2002], some passive margins cannot be considered only to be inert sites of sedimentation and progressive subsidence. They provide several examples of such passive margins and describe their results on the Kwanza basin, Angola, which is located in a very stable intraplate region. *Leroy* [2004] studied mechanisms of postrifting compressional deformation of numerous passive margins (i.e., Norway, Greenland, West Africa, Brazil, India, Australia etc. . .). Various mechanisms have been invoked to explain their reactivation. Through thermomechanical modeling, we show that the Ligurian Sea is a good place to study the coeval influence of these different parameters on the reactivation of its passive margins.

8.1. Thermal Effects

[45] *Assumpçao et al.* [2004] explain the stress concentration in SE Brazil (including a part of the passive margin) as resulting from the thermal effect of a locally shallower asthenosphere. *Hudec and Jackson* [2002] also postulated thermal effects to explain the reactivation of the Kwanza basin. *Leroy et al.* [2004] show that the postrifting deformation of passive margins can induce uplift of the continental hinterland.

[46] Considering the thermal modeling of the Ligurian Basin, Figures 5a and 5b show that the basin is still cooling, because of the lithosphere has not yet reached its equilibrium thickness. The isotherms are deflected on the two flanks of continental margins. The consequence is the combined effects of the thermal expansion that uplift the flanks and the thermal contraction that subsides the cooling lithosphere of the adjacent basin.

[47] These processes generate stresses into the lithosphere. This could generate low compressive movements and low levels of deformation. Our numerical tests respect to the thermal parameters show that these thermal effects have a main influence on the amount of deformation. The strain can vary in a ratio of tens according the choice of these values.

8.2. Buoyancy Forces

[48] The different tests (e.g., the slope of the Moho) allow concluding that gravitational forces has also a strong influence in the deformation at the foot of the margins. We note that the topography changes from 3000 m down to −2500 m within around 100 km of horizontal distance, and correlatively, on the same distance, the Moho depth changes from 50 km under the internal Alps, north of Argentera massif [*Thouvenot et al.*, 2007] up to 12.5 km in the center of the basin. In comparison to surrounding regions, this deformation is strongly localized. Because of the asymmetry of the two surrounding continental lithospheres these body forces are larger on the Alpine side (northern margin) than on the Corsican side, enhancing the asymmetry of thermal effects. The strain rate is also more important toward the northeast of the basin (cross section B) because the topographic contrast is sharper than along the Profile A, which describes the central part of the basin.

8.3. Influence of Rheological Parameters

[49] We also show the influence of rheological parameters on the amount of localized stress.

[50] Previously, *Gölke et al.* [1996] carried out a finite element modeling of stress patterns along the mid-Norwegian continental margin, under the far-field effect of ridge-push. They concluded that the stress anisotropy, observed in the area is first linked to a contrast across in rheology between the continental margin and the oceanic margin, but these stress deviations are also related to topographic variation, inducing gravitationally compression.

[51] In our study case, the modeling of the Ligurian margins, the rheology contrast between continental and oceanic lithosphere is not the main factor explaining concentration of deformation at the foot of the margin. The strain varies in a ratio of 20% if we take into account or not the presence of oceanic-type crust.

[52] We also show that the blanketing of the sedimentary layer favors the deflection of heat toward the foot of the margin but also strongly decreases the amount of strain, when this thickness increases.

8.4. Tectonic Forces

[53] The results that we obtained with negligible tectonic forces but only realistic thermal effects and gravity forces provide weak values of deformation, that can hardly explain the occurrence of magnitude 6 earthquakes.

[54] Using the seismic moments of the biggest recorded events, between 1963 and 1995, *Béthoux et al.* [1998] deduced a shortening deformation of about 1.3×10^{-8} a^{-1} (0.4110^{-15} s^{-1}) over a distance of 80 km in a southeastern direction. The modeled total strain obviously depends also on the velocity shortening applying to the boundary. Using the rheological parameters (Table 1), and velocity from 0.1 up to 0.5 mm a^{-1} (following the GPS results) we obtain a averaged cumulative strain rate (ranging from 10^{-15} s^{-1} up 10^{-14} s^{-1}), in the order of magnitude of the strain deduced from seismic moments.

[55] According to our numerical tests, we conclude that these tectonic forces are necessary to obtain a deformation in agreement with the seismic strain quantification. These very low boundary stress forces are locally amplified by the previously described factors: thermal features, buoyancy forces and contrasts in rheology.

[56] Correlatively, taking into account the uncertainties of both evaluations, this fact allows postulating that a notable amount of deformation is accommodated by seismic activity.

[57] At the difference of typical passive margin, no action of ridge-push is acting in Mediterranean. Here, topographic

effect and low boundary stress come from the surrounding mountainous.

[58] However, no simple model can explain all aspects of such reactivation in a compressive pattern. Particularly, our modeling does not implement the role of inherited structures such as transform faults or synrift normal faults that probably act to favor weakness of this margin.

[59] We also note that our models compute deformation localized at the foot of the northern margin, without using different rheology parameters for southern and northern modeled crustal blocks. However, *Burrus et al.* [1987] proposed that the northern margin should be weaker than the southern margin as a consequence of the reconstitution of the complex drifting phase, leading to the formation of the Liguro-Provençal basin. In this case, the deformation of the northern margin should be larger than this evaluated in the modeling.

9. Conclusion: Why is the Ligurian Basin Seismogenic? Geodynamical Implications

[60] In conclusion, the stress amplification in this marginal basin is both due to its peculiar geometric conditions, narrow and with a thick hinterland region (Alps and Corsica) and to the high temperature of the basin that has not yet reached its thermal equilibrum after rifting process. Because of the instability of the thickened continental lithosphere, small compression forces on the rim of the Alpine belt, are both sufficient and necessary to initiate the collapse of this continental crust in the topographic low forming the Ligurian Basin.

[61] Present-day compressive stress fields act at the boundary of the Alpine system [*Eva and Solarino*, 1998; *Calais et al.*, 2002; *Delacou et al.*, 2004a, 2004b; *Jimenez-Munt et al.*, 2005; *Sue et al.*, 2007] as far as the Provençal region [*Chardon and Bellier*, 2003; *Cushing et al.*, 2008]. Here, we shall not discuss the origin of this stress (only due to buoyancy effect or linked to a rotation between Apulia and Europe, depending of the point of view of these different authors). No evidence of deformation (neither seismicity, nor observation in seismic profiles) can be made in the southern margin. The Corsica-Sardinia block is also quasi aseismic and appears rigidly attached to stable Europe, according GPS data [*Nocquet and Calais*, 2004].

[62] We therefore propose that the low compressive forces deduced by these different studies are locally accommodated by compressive seismic activity in the northern margin of the Ligurian Basin. This mechanical scenario and its correlative thermal features, linked to a high heat flow, consequence of a drifting-rifting episode, explain the rather shallow seismic activity (5–11 km depth) located at the foot of the northern margin. These events reactive inherited faulting linked to the rifting. Occurrence of slightly deeper (up to 20 km deep) earthquakes near the center of the basin is more likely favored by contrast in rheology and by the presence of a transfer zone, originally identified on the margin by *Rollet et al.* [2002], that accommodates the differential deformation between two segments of the margin.

[63] The corresponding modeled strain rate is in good agreement with the historical as well as with the accurately located instrumental seismicity pattern, improving the degree of confidence we can have in determining the regional seismic hazard.

[64] **Acknowledgments.** We are particularly indebted to J. P Rehault who taught us a lot about the Mediterranean Sea and Ligurian Basin. We thank J. M. Nocquet and G. Nolet for helpful discussions. We are grateful to S. Solarino who kindly provided us his seismic events location file. Both anonymous reviewers and the associated editor helped us to improve the initial version of this paper. This study was supported by Institut Français des Sciences de l'Univers (INSU/CNRS) under ACI "IRIS" project.

References

Assumpçao, M., M. Schimmel, C. Escalante, J. R. Barbosa, M. Rocha, and L. V. Barros (2004), Intraplate seismicity in SE Brazil: Stress concentration and lithospheric thin spots, *Geophys. J. Int.*, *159*, 390–399, doi:10.1111/j.1365-246X.2004.02357.x.

Baroux, E., N. Béthoux, and O. Bellier (2001), Analyses of the stress field in southeastern France from earthquake focal mechanisms, *Geophys. J. Int.*, *145*, 336–348, doi:10.1046/j.1365-246x.2001.01362.x.

Bertil, D., N. Béthoux, M. Campillo, and B. Massinon (1989), Modeling crustal phases in southeast France for focal depth determination, *Earth Planet. Sci. Lett.*, *95*, 341–358, doi:10.1016/0012-821X(89)90109-X.

Béthoux, N., J. Fréchet, F. Guyoton, F. Thouvenot, M. Cattaneo, C. Eva, B. Feignier, M. Nicolas, and M. Granet (1992), A closing Ligurian Sea?, *Pure Appl. Geophys.*, *139*, 179–194, doi:10.1007/BF00876326.

Béthoux, N., G. Ouillon, and M. Nicolas (1998), The instrumental seismicity of the Western Alps: Spatio-temporal patterns analysed with the wavelet transform, *Geophys. J. Int.*, *135*, 177–194, doi:10.1046/j.1365-246X.1998.00631.x.

Bigot-Cormier, F., F. Sage, M. Sosson, J. Deverchère, M. Ferrandini, P. Guennoc, M. Popoff, and J. F. Stéphan (2004), Déformation pliocènes de la marge nord-Ligure: Les conséquences d'un chevauchement crustal sud-alpin, *Bull. Soc. Geol. Fr.*, *175*(2), 197–211, doi:10.2113/175.2.197.

Boschi, E., G. Ferrari, P. Gasperini, E. Guidoboni, G. Smriglio, and G. Valensise (1995), Catalogo dei forti terremoti in Italia dal 461 a.C. al 1980, report, 973 pp., Ist. Naz. di Geofis., Bologna, Italy.

Burrus, J., F. Bessis, and B. Doligez (1987), Heat flow, subsidence and crustal structure of the Gulf of Lion (NW Mediterranean): A quantitative discussion of the classical passive margin model, in *Sedimentary Basins and Basin-Forming Mechanisms*, vol. 12, edited by C. Beaumont and A. J. Tankart, pp. 1–15, Can. Soc. of Pet. Geol., Calgary, Alberta.

Byerlee, J. (1978), Friction of rocks, *Pure Appl. Geophys.*, *116*, 615–626, doi:10.1007/BF00876528.

Calais, E., L. Galisson, J. F. Stéphan, J. Delteil, J. Deverchère, C. Larroque, B. Mercier de Lépinay, M. Popoff, and M. Sosson (2000), Crustal strain in the Southern Alps, 1948–1998, *Tectonophysics*, *319*, 1–17, doi:10.1016/S0040-1951(00)00029-9.

Calais, E., J. M. Nocquet, F. Jouanne, and M. Tardy (2002), Current strain regime in the Western Alps from continuous GPS measurements, *Geology*, *30*(7), 651–654, doi:10.1130/0091-7613(2002)030<0651:CSRITW>2.0.CO;2.

Capponi, G., C. Eva, and F. Merlanti (1980), Il terremoto del 23 Febbraio 1887 in Liguria occidentale, *Atti Accad. Ligure Sci. Lett. Genoa*, *37*, 1–33.

Chamot-Rooke, N., J. M. Gaulier, and F. Jestin (1999), Constraints on Moho depth and crustal thickness in the Liguro-Provençal Basin from a 3D gravity inversion: Geodynamic implications, *Geol. Soc. Spec. Publ.*, *156*, 37–61.

Chardon, C., and O. Bellier (2003), Geological boundary conditions of the 1909 Lambesc (Provence, France) earthquake: Structure and evolution of the Trévaresse ridge anticline, *Bull. Soc. Geol. Fr.*, *174*(5), 497–510, doi:10.2113/174.5.497.

Chaumillon, E., J. Deverchère, J. P. Réhault, and E. Gueguen (1994), Réactivation tectonique et flexure de la marge continentale Ligure (Méditerranée occidentale), *C. R. Acad. Sci., Ser. II*, *319*, 675–682.

Chen, Y., and J. W. Morgan (1990), A nonlinear rheology model for mid-ocean ridge axis topography, *J. Geophys. Res.*, *95*, 17,583–17,604, doi:10.1029/JB095iB11p17583.

Chery, J., M. D. Zoback, and R. Hassani (2001), An integrated mechanical model of the San Andreas fault in central and northern California, *J. Geophys. Res.*, *106*, 22,051–22,066, doi:10.1029/2001JB000382.

Contrucci, I., A. Nercessian, A. Mauffret, N. Béthoux, and G. Pascal (2001), A Ligurian (Western Mediterranean Sea) geophysical transect revisited, *Geophys. J. Int.*, *146*, 74–97, doi:10.1046/j.0956-540x.2001.01418.x.

Courboulex, F., A. Deschamps, M. Cattaneo, F. Costi, J. Deverchere, J. Virieux, P. Augliera, V. Lanza, and D. Spallarossa (1998), Source study and tectonic implications of the 1995 Ventimiglia (border of Italy and France) earthquake (M_L = 4.7), *Tectonophysics*, *290*, 245–257, doi:10.1016/S0040-1951(98)00024-9.

Courboulex, F., et al. (2007), Seismic hazard on the French Riviera: Observations, interpretations and simulations, *Geophys. J. Int.*, *170*, 387–400, doi:10.1111/j.1365-246X.2007.03456.x.

Cushing, E. M., O. Bellier, S. Nechtschein, M. Sébrier, A. Lomax, P. Volant, P. Dervin, P. Guignard, and L. Bove (2008), A multidisciplinary study of a slow-slipping fault for seismic hazard assessment: The example of the Middle Durance Fault (SE France), *Geophys. J. Int.*, *172*, 1163–1178, doi:10.1111/j.1365-246X.2007.03683.x.

Delacou, B., C. Sue, J. D. Champagnac, and M. Burkhard (2004a), Present-day geodynamics in the bend of the Western and central Alps as constrained by earthquakes analysis, *Geophys. J. Int.*, *158*, 753–774, doi:10.1111/j.1365-246X.2004.02320.x.

Delacou, B., C. Sue, J. D. Champagnac, and M. Burkhard (2004b), Origin of the current stress field in the Western/central Alps: Role of gravitational reequilibration constrained by numerical modelling, *J. Geol. Soc. London*, *243*, 295–310.

Della Vedova, B., F. Lucazeau, V. Pasquale, G. Pellis, and M. Verdoya (1995), Heat flow in the tectonic provinces crossed by the southern segment of the European geotraverse, *Tectonophysics*, *244*, 57–74, doi:10.1016/0040-1951(94)00217-W.

Doglioni, C., E. Gueguen, F. Sabat, and M. Fernandez (1997), The western Mediterranean extensional basins and the Alpine orogen, *Terra Nova*, *9*(3), 109–112.

Eva, E., and S. Solarino (1998), Variations of stress directions in the western Alpine arc, *Geophys. J. Int.*, *135*, 438–448, doi:10.1046/j.1365-246X.1998.00649.x.

Eva, E., S. Solarino, and D. Spallarossa (2001), Seismicity and crustal structure beneath the western Ligurian Sea derived from local earthquake tomography, *Tectonophysics*, *339*, 495–510, doi:10.1016/S0040-1951(01)00106-8.

Faccenna, C., C. Piromallo, A. Crespo-Blanc, L. Jolivet, and F. Rossetti (2004), Lateral slab deformation and the origin of the western Mediterranean arcs, *Tectonics*, *23*, TC1012, doi:10.1029/2002TC001488.

Ferrari, G. (1991), The 1887 Ligurian earthquake: A detailed study from contemporary scientific observations, *Tectonophysics*, *193*, 131–139, doi:10.1016/0040-1951(91)90194-W.

Ginzburg, A., J. Makris, and R. Nicolich (1986), European geotraverse: A seismic refraction profile across the Ligurian Sea, *Tectonophysics*, *126*, 85–97, doi:10.1016/0040-1951(86)90221-0.

Goes, S., D. Giardini, S. Jenny, C. Hollenstein, H.-G. Kahle, and A. Geiger (2004), A recent tectonic reorganization in the South Central Mediterranean, *Earth Planet. Sci. Lett.*, *226*, 3–4.

Gölke, M., S. Cloeting, and D. Coblentz (1996), Finite-element modelling of stress patterns along the mid-Norwegian continental margin, 62° to 68°N, *Tectonophysics*, *266*, 33–53, doi:10.1016/S0040-1951(96)00182-5.

Gueguen, E., C. Doglioni, and M. Fernandez (1997), Lithospheric boudinage in the Western Mediterranean back-arc basins, *Terra Nova*, *9*(4), 184–187, doi:10.1046/j.1365-3121.1997.d01-28.x.

Gueguen, E., C. Doglioni, and M. Fernandez (1998), On the post-25 Ma geodynamic evolution of the western Mediterranean, *Tectonophysics*, *298*, 259–269, doi:10.1016/S0040-1951(98)00189-9.

Hansen, D. L., and S. B. Nielsen (2002), Does thermal weakening explain basin inversion? Stochastic modelling of the thermal structure beneath sedimentary basins, *Earth Planet. Sci. Lett.*, *198*, 113–127, doi:10.1016/S0012-821X(02)00471-5.

Hassani, R., D. Jongmans, and J. Chéry (1997), Study of plate deformation and stress in subduction processes using two-dimensional numerical models, *J. Geophys. Res.*, *102*, 17,951–17,965, doi:10.1029/97JB01354.

Hudec, M. R., and M. P. A. Jackson (2002), Structural segmentation, inversion, and salt tectonics on a passive margin: Evolution of the inner Kwansa Basin, Angola, *Geol. Soc. Am. Bull.*, *114*, 1222–1244, doi:10.1130/0016-7606(2002)114<1222:SSIAST>2.0.CO;2.

Jemsek, J., R. Von Herzen, J.-P. Rehault, D. L. Williams, and J. Sclater (1985), Heat flow and lithospheric thinning in the Ligurian Basin (N.W. Mediterranean), *Geophys. Res. Lett.*, *12*, 693–696, doi:10.1029/GL012i010p00693.

Jimenez-Munt, I., D. Garcia-Castellanos, A. M. Negredo, and J. P. Platt (2005), Gravitational and tectonic forces controlling postcollisional deformation and the present-day stress field of the Alps: Constraints from numerical modeling, *Tectonics*, *24*, TC5009, doi:10.1029/2004TC001754.

Jolivet, L., and C. Faccenna (2000), Mediterranean extension and the Africa-Eurasia collision, *Tectonics*, *19*(6), 1095–1107, doi:10.1029/2000TC900018.

Jolivet, L., R. Dubois, M. Fournier, B. Goffé, A. Richard, and C. Jourdan (1990), Ductile extension in Alpine Corsica, *Geology*, *18*(10), 1007–1010, doi:10.1130/0091-7613(1990)018<1007:DEIAC>2.3.CO;2.

Kirby, S. (1985), Rocks mechanics observations pertinent to the rheology of the lithosphere and the localization of strain along shear zones, *Tectonophysics*, *119*, 1–27, doi:10.1016/0040-1951(85)90030-7.

Leroy, M. (2004), Mécanismes de déformation post-rifting des marges passives, Exemple des marges péri-Atlantiques et modélisation, Ph.D. thesis, 244 pp., Univ. of Rennes, Rennes, France.

Leroy, Y., and M. Ortiz (1989), Finite element analysis of strain localization in frictional materials, *Int. J. Numer. Anal. Methods Geomech.*, *13*, 53–74, doi:10.1002/nag.1610130106.

Leroy, M., O. Dauteuil, and P. R. Cobold (2004), Incipient shortening of a passive margin: The mechanical roles of continental and oceanic lithospheres, *Geophys. J. Int.*, *159*, 400–411, doi:10.1111/j.1365-246X.2004.02400.x.

McKenzie, D. P. (1972), Active tectonics of the Mediterranean region, *Geophys. J. R. Astron. Soc.*, *30*, 153–160.

McKenzie, D. P. (1978), Some remarks on the development of sedimentary basins, *Earth Planet. Sci. Lett.*, *18*, 1–32.

Nocquet, J. M., and E. Calais (2003), Crustal velocity field of western Europe from permanent GPS array solutions, 1996–2001, *Geophys. J. Int.*, *154*, 72–88, doi:10.1046/j.1365-246X.2003.01935.x.

Nocquet, J. M., and E. Calais (2004), Geodetic measurements of crustal deformation in the Western Mediterranean and Europe, *Pure Appl. Geophys.*, *161*, 661–681.

Panza, G. F., S. Mueller, and G. Calcagnile (1980), The gross feature of the lithosphere-asthenosphere system in Europe from seismic surface waves and body waves, *Pure Appl. Geophys.*, *118*, 1209–1213, doi:10.1007/BF01593061.

Pasquale, V., M. Verdoya, and P. Chiozzi (1996), Heat flux and timing of the drifting stage in the Ligurian-Provençal basin (northwestern Mediterranean), *J. Geodyn.*, *21*(3), 205–222, doi:10.1016/0264-3707(95)00035-6.

Rehault, J. P., G. Boillot, and A. Mauffret (1984), The western Mediterranean basin: Geological evolution, *Mar. Geol.*, *55*, 447–477, doi:10.1016/0025-3227(84)90081-1.

Rollet, N. (1999), Structures profonde et dynamique du Bassin Ligure et de ses marges, Ph.D. thesis, 292 pp., Univ. of Paris VI, Paris.

Rollet, N., J. Deverchère, M. O. Beslier, P. Guennoc, J. P. Réhault, M. Sosson, and C. Truffert (2002), Back arc extension, tectonic inheritance, and volcanism in the Ligurian Sea, Western Mediterranean, *Tectonics*, *21*(3), 218–243, 1015, doi:10.1029/2001TC900027.

Royden, L., and C. E. Keen (1980), Rifting processes and thermal evolution of the continental margin of eastern Canada determined from subsidence curves, *Earth Planet. Sci. Lett.*, *51*, 343–361, doi:10.1016/0012-821X(80)90216-2.

Sandwell, D. T., and W. H. F. Smith (1995), Marine gravity anomaly from satellite altimetry, map, Scripps Inst. of Oceanogr., La Jolla, Calif.

Savoye, B., and J. Piper (1991), Quaternary sea-level change and sedimentation on the continental shelf and slope of Antibes, French Riviera, *Geo Mar. Lett.*, *13*, 3–8.

Sclater, J. G., L. Royden, F. Horvath, B. C. Burchfiel, S. Semken, and L. Stegena (1980), The formation of the intra-Carpathian basins as determined from subsidence data, *Earth Planet. Sci. Lett.*, *51*, 139–162, doi:10.1016/0012-821X(80)90262-9.

Scotti, O., et al. (2007), Définition de scénarii sismiques pour la région de Nice, France, paper presented at 7th National Symposium, Assoc. Fr. de Génie Para-Sismique, Paris, 4–6 Jul.

Selvaggi, G., and A. Amato (1992), Intermediate-depth earthquake in northern Apennines (Italy): Evidence of a still active subduction?, *Geophys. Res. Lett.*, *19*, 2127–2130, doi:10.1029/92GL02503.

Serpelloni, E., M. Anzidei, P. Baldi, G. Casula, and A. Galvani (2005), Crustal velocity and strain-rate fields in Italy and surrounding regions: New results from the analysis of permanent and non-permanent GPS networks, *Geophys. J. Int.*, *161*, 861–880, doi:10.1111/j.1365-246X.2005.02618.x.

Solarino, S., D. Spalarossa, S. Parolia, M. Cattaneo, and C. Eva (1996), Litho-asthenospheric structures of northern Italy as inferred from teleseismic P wave tomography, *Tectonophysics*, *260*, 271–289, doi:10.1016/0040-1951(95)00201-4.

Sue, C., F. Thouvenot, J. Frechet, and P. Tricart (1999), Widespread extension in the core of the Western Alps revealed by earthquake analysis, *J. Geophys. Res.*, *104*, 25,611–25,622, doi:10.1029/1999JB900249.

Sue, C., B. Delacou, J. D. Champagnac, C. Allanic, and M. Burkhard (2007), Aseimic deformation in the Alps: GPS vs. seismic strain quantification, *Terra Nova*, *19*(3), doi:doi:10.1111/j.1365-3121.2007.00732.x.

Thouvenot, F., A. Paul, J. Fréchet, N. Béthoux, L. Jenatton, and R. Guiguet (2007), Are there really superposed Mohos in the south-western Alps? New seismic data from fan-profiling reflections, *Geophys. J. Int.*, *170*, 1180–1194, doi:10.1111/J.1365-246X.2007.03463.x.

Vigny, C., et al. (2002), GPS network monitors the Western Alps over a five year period: 1993–1998, *J. Geod.*, *76*, 63–76, doi:10.1007/s00190-001-0231-8.

Waldhauser, F., E. Kissling, and S. Mueller (1998), Three-dimensional interface modelling with two-dimensional seismic data: The Alpine crust-mantle boundary, *Geophys. J. Int.*, *135*, 264–278, doi:10.1046/j.1365-246X.1998.00647.x.

Zito, G. (2005), Heat flow anomaly and lithospheric thinning of the Tuscan extensional back-arc basin (Italy), *J. Geodyn.*, *40*(1), 1–22, doi:10.1016/j.jog.2005.04.001.

M.-O. Beslier, N. Béthoux, and E. Tric, Géosciences Azur, Université de Nice, B.P. 48, F-06235 Villefranche sur Mer, France. (beslier@geoazur.obs-vlfr.fr; nbethoux@geoazur.obs-vlfr.fr; tric@geoazur.unice.fr)

J. Chery, Laboratoire de Géophysique et Tectonique, Université Montpellier II, CNRS, Place E. Bataillon, F-34000 Montpellier, France. (chery@univ-montp2.fr)